

1 **Experimental study of viscosity and thermal conductivity of water based Fe₃O₄ nanofluid**
2 **with highly disaggregated particles**

3 *Zeyu Liu^{1,2}, Xin Wang², Hongtao Gao¹, Yuying Yan^{2*}*

4 *1. Marine Engineering College, Dalian Maritime University, Dalian, 116026, China*

5 *2. Fluids & Thermal Engineering Research Group, Faculty of Engineering, the*
6 *University of Nottingham, Nottingham NG7 2RD, UK*

7
8 **Corresponding author: yuying.yan@nottingham.ac.uk*

9
10 **Abstract**

11 This work aims to experimentally study the viscosity and thermal conductivity of water based
12 Fe₃O₄ nanofluid with highly disaggregated nanoparticles. The citric acid is modified on Fe₃O₄
13 nanoparticles with carboxyl groups, which enables particles to be disaggregated by enhancing
14 the surface potential of nanoparticles through increasing pH values. To study the highly
15 disaggregated Fe₃O₄ nanofluid, we firstly investigate the effect of volume fraction, pH value,
16 and temperature on the viscosity of modified Fe₃O₄ nanofluid. The experimental results show
17 that the viscosity of the modified Fe₃O₄ nanofluid is in good agreement with the Einstein
18 equation when nanoparticles are highly disaggregated. At a pH of 8, We then study the effect
19 of volume fraction and temperature on the thermal conductivity of modified Fe₃O₄ nanofluid.
20 While the enhancement of modified Fe₃O₄ nanofluid is not significant, the highest thermal
21 conductivity can be achieved when nanofluid is at a highly disaggregated level with a volume
22 fraction of 0.32%, and thermal conductivity is consistent with the classic Maxwell model.

23 **Keywords:** nanofluid, disaggregation, viscosity, thermal conductivity, zeta potential, pH

24

25 Introduction

26 Nanofluid is defined as a nano-size suspension, and nanoparticles (1-100nm) are typically
27 made of metal, metal oxide and semi-conductor. Traditionally, heat transfer liquids, which
28 include water, oil and ethylene glycol mixture, are used as a base liquid to disperse particles
29 and make the suspension flowable. Since Choi et al. [1] has introduced nanofluids in 1995, a
30 large number of repetitive experiments demonstrated the effectiveness of nanofluids in
31 thermophysical properties. Many similar reports also proved the significant enhancement of
32 thermal conductivity of a nanofluid was caused by the increasing volume fraction. Among
33 them, Philip et al. [2] even experimentally observed a 300% enhancement of thermal
34 conductivity from a Fe_3O_4 nanofluid which is with a volume fraction of 6.3%.

35 However, aggregation is a significant challenge that impedes the practical application of
36 nanofluids. It is widely accepted that magnetic nanoparticles have a great tendency to
37 aggregate in the solution due to van Der Waals force of attraction [3]. When nanoparticles
38 undergo aggregation, the effective volume fraction of particle aggregates is greater than that
39 of isolated particles. Therefore, the viscosity of nanofluid will increase, which makes nanofluid
40 behave like a non-Newtonian fluid [4]. There are two common approaches to control particle
41 aggregation in the engineering field, which include long-time ultrasonic treatment and
42 surfactants. Long-time ultrasonic treatment can break large aggregates. Although short-term
43 stability can be achieved after ultrasonic treatment, aggregation is still inevitable if colloidal
44 stability is poor. Colloidal stability depends on electrostatic repulsion and steric effect [3]. The
45 electrostatic repulsion is based on the increasing electric repulsive force between
46 nanoparticles that are with the charges of the same sign. The steric effect stabilises a particle
47 by coating it with a large molecule so that the particles cannot get too close to each other.
48 Surfactants stabilise particles via enhancing one or both, depending on the molecular size of
49 the surfactant and its type. Surfactants stay at the surface of particles by physical absorption.
50 To favour the absorption kinetic, there must be a large number of free surfactants dispersing
51 in the liquid phase. However, these free surfactants produce foams during heating and
52 pumping. Moreover, adding a solvent of low polarity (i.e. anti-freezer ethylene glycol) will
53 also trigger the desorption of surfactant [5], making worse the colloidal stability. Therefore, a
54 stable and surfactant-free nanofluid with predictable thermal physical properties should be
55 much more promising for the enhancement of heat transfer.

56 Additionally, shear thinning is a phenomenon characteristic of non-Newtonian fluids in which
57 the viscosity of fluid decreases with the increase of shear rate during rheological
58 measurements. Zhou et al. [6] made a hypothesis that the reduction of viscosity at a high
59 shear rate was caused by particle aggregates being broken under shear force. This hypothesis
60 well explains why shear thinning often becomes more obvious with the increase of particle
61 volume fraction [7, 8]. Pastoriza-Gallego et al. [9] studied the viscoelastic behaviour of Fe_2O_3
62 nanofluids. They observed a peak showing on the profile of loss modulus against strain. They
63 interpreted the peak as some kinds of the structures formed by particles within the fluid that
64 is lost during the increase of strain. If shear thinning of nanofluid has to do with the aggregates

65 being broken under shear, the nanoparticles which are highly dispersed should make the
66 viscosity less dependent on shear rate. Prasher et al. [10] theoretically related the viscosity of
67 nanofluid to the size of particle aggregates by modifying Krueger and Dougherty's model.
68 They predicted that the viscosity decreases by reducing the size of particle aggregates and
69 the viscosity should be consistent with the classic Einstein equation [11] after particles are
70 completely disaggregated. However, it is still suspected that the Einstein equation is effective
71 when nanoparticles become highly disaggregated.

72 The enhanced thermal conductivity of nanofluid is also an attractive feature for researchers
73 in thermal engineering. Abareshi et al. [12] found an 11.5% enhancement in the thermal
74 conductivity of water based Fe_3O_4 nanofluid at 40°C after the volume fraction was increased
75 to 3%. Singh et al. [13] found that the thermal conductivity of Fe_3O_4 nanofluid increased by
76 33%-46% at 60°C when particle volume fraction was 2%. Although the thermal conductivity
77 of nanofluid increases by adding more nanoparticles, lots of evidence also demonstrates the
78 mismatch between the experimental results and the data calculated by established
79 theoretical models [14-17]. Bigdeli et al. [18] suggested that most enhancements beyond
80 predictions of effective medium theories were caused by the formation of thermal
81 percolating paths, which is due to the aggregation of nanoparticles [19-21]. Prasher et al. [2]
82 reported that there should be an optimal aggregated scale to enhance the thermal
83 conductivity of nanofluid by modelling the contribution of aggregations to thermal
84 conduction. They found that both fully aggregated and well-dispersed nanofluid should
85 generate thermal conductivity comparable to that predicted by the Maxwell model. If the
86 particles undergo uncontrolled aggregation, no models can predict the thermal conductivity
87 of nanofluid.

88 The present work aims to investigate the effect of particle disaggregation on the viscosity and
89 thermal conductivity of water based Fe_3O_4 nanofluid. Citric acid, as a modification, is used to
90 cover the surfaces of the prepared Fe_3O_4 nanoparticles with carboxyl groups so that
91 disaggregation can be promoted by improving the surface potential of the particles through
92 increasing pH values. It has been suggested that the Light scattering technique is a good
93 approach to characterise the aggregation condition of nanofluids [22]. Thus, DLS (dynamic
94 light scattering) measurement is carried out to investigate the disaggregation at different pH
95 values. Rheological measurement is conducted to figure out the relationship between
96 viscosity and particle concentration at different temperatures. Moreover, at a pH of 8, we
97 also studied the effect of volume fraction and temperature on the thermal conductivity of
98 Fe_3O_4 nanofluid. In this work, the experimental results of both viscosity and thermal
99 conductivity of Fe_3O_4 nanofluid are compared with the Einstein equation and the Maxwell
100 equation, respectively.

101 **Methods**

102 **Synthesis of citric acid modified Fe₃O₄ nanofluid**

103 Fe₃O₄ nanoparticles are synthesised by the co-precipitation method. In a typical procedure,
104 8.8 g FeCl₂·4H₂O (≥99%, Sigma Aldrich) and 24 g FeCl₃·6H₂O (≥99%, Sigma Aldrich) are added
105 into 100 ml water at first. The suspension is stirred at 50°C and bubbled under the protection
106 of N₂ for 2 hours to remove O₂. 50 ml of ammonium hydroxide (25%, Sigma Aldrich) is then
107 dissolved under vigorous stirring for 30 minutes. The black precipitate is magnetised to the
108 bottom of the flask and washed with HCl solution (37%, Sigma Aldrich) for 5 times. 30 minutes
109 later, after dumping the supernatant, the prepared precipitate is dissolved into 120 ml water
110 by ultrasonic treatment. To cover particle surfaces with carboxyl groups, particles are coated
111 with citric acid (≥99.5%, Sigma Aldrich) which is a small molecule with three carboxyl groups.
112 Citric acid can be chemically attached to the surface of a nanoparticle via the formation of a
113 coordination bond between a metal atom and a carboxyl group, leaving one or two carboxyl
114 groups stretching out forward into the surrounding liquid phase [23]. Finally, a certain number
115 of coated nanoparticles in an aqueous solution are dispersed into DI water.

116 **Characterisations**

117 TEM (Transmission electron microscopy) images are captured under an electron microscope
118 (JEOL-2000) operating at 200kV. The samples for the TEM test are prepared by dropping
119 diluted particle dispersion onto a TEM copper grid followed by drying overnight. XRD (X-ray
120 powder diffraction) pattern is carried out by applying a Bruker D8 Advance Powder X-ray
121 diffractometer. TGA (Thermogravimetric analysis) is conducted by using a TGA- SDTQ600
122 thermogravimetric analyser. The citric acid modified Fe₃O₄ nanoparticles are heated at
123 1000°C with the protection of Nitrogen. The heating temperature increases remaining at 10°C
124 per minute. The density of modified and unmodified Fe₃O₄ nanoparticles is measured by using
125 an Occupy 1330 pycnometer. Before the test, the particle sample is dried under reduced
126 pressure for 3 days. The equipment is calibrated by conducting 10 purges and 10 runs for the
127 empty cell followed by 10 purges and 10 runs for the cell and two calibration balls. Zeta
128 potential and dynamic light scattering measurements are obtained by a Zetasizer (Malvern
129 Zen 3600). All samples prepared for zeta potential and dynamic light scattering are diluted to
130 0.002 vol.% and then pH is adjusted to the desired value. The samples are sonicated for 2-3
131 minutes prior to each measurement.

132 Typically, the viscosity of the prepared samples is tested under the shear rate from 50 to 2500
133 s⁻¹, respectively at a specific temperature. For every measurement, the shear rates are carried
134 out under stable shear conditions for 2 minutes. The measurement of the viscosity is captured
135 every 6 seconds and the average viscosity is defined as the viscosity at a fixed shear rate.
136 Additionally, final viscosity of the prepared sample at a certain volume fraction and
137 temperature is calculated by averaging the viscosity of each shear rate.

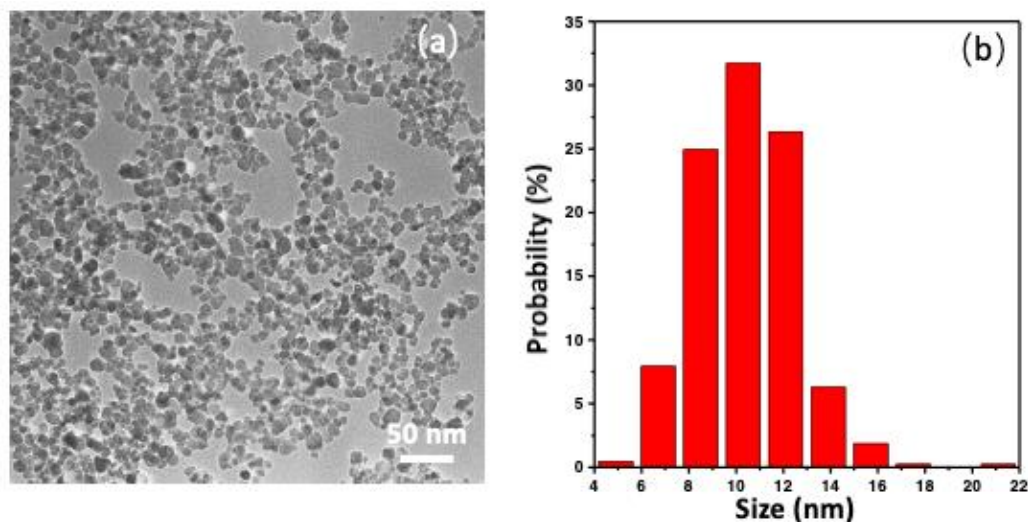
138 In terms of the thermal conductivity of the modified Fe₃O₄ nanofluid, it is measured by a
139 TC3020 Liquid thermal conductivity meter (Xi'an Xiotech Electronic Technology Co., China),

140 the thermal conductivity meter is based on the transient hot-wire method. A water bath is
141 used to generate a circulation flow to maintain the sample at a certain temperature during
142 the measurement. After setting the temperature for a test, the sample needs to be heated
143 for over half an hour to achieve thermal stabilisation. Finally, the thermal conductivity is
144 measured 5 times to obtain the mean value.

145 Results and discussion

146 Characterisations of Fe₃O₄ nanoparticles

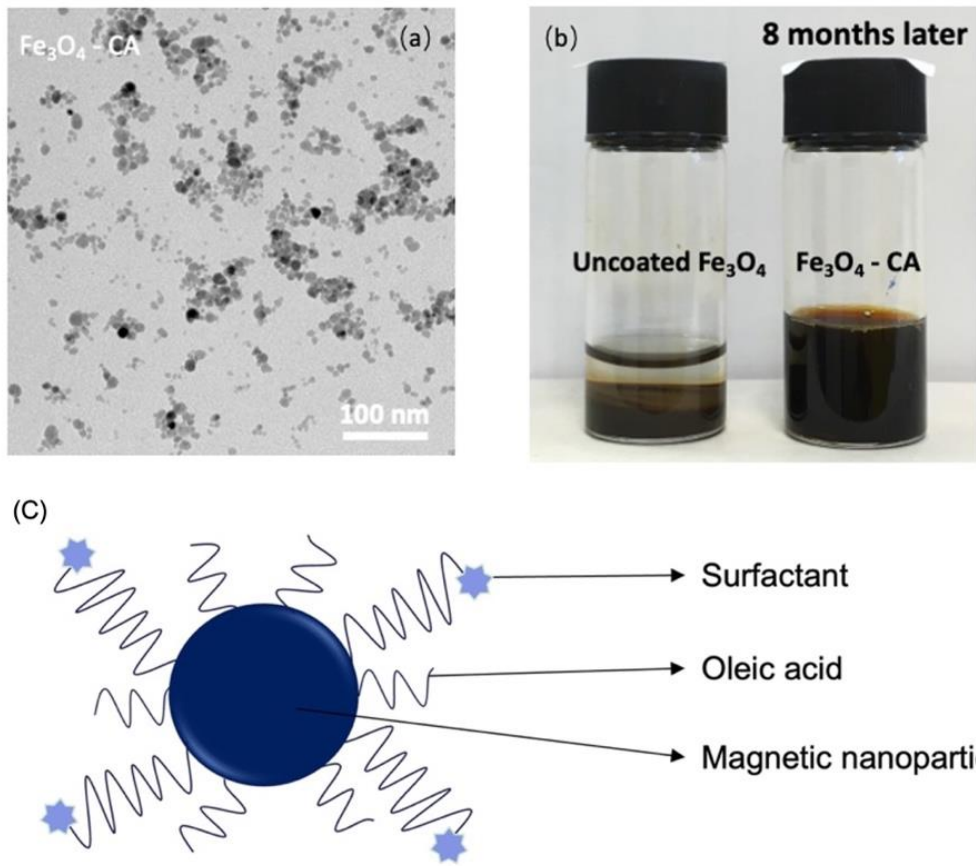
147 Fig. 1 presents the TEM image and the size distribution of bare Fe₃O₄ nanoparticles that are
148 synthesised by the co-precipitation approach. The nanoparticles are spheric in shape. As
149 shown in Fig. 1(b), the size distribution of nanoparticles ranges from 4 to 22 nm, and the
150 average size of the nanoparticles is approximately 10 nm. To cover the surfaces of bare
151 particles with carboxyl groups, the particles are modified with citric acid which is a small
152 molecule with three carboxyl groups. It can be chemically attached to the surface of particles
153 via the formation of a coordinate bond between the metal atom and carboxyl group (Fig. 2(c)),
154 leaving carboxyl groups stretching out forward into the surrounding liquid phase [24]. These
155 free carboxyl groups are expected to dissociate, generating a negatively charged group COO⁻
156 on the surface of the particle. To test the colloidal stability of modified particles, nanofluids
157 with both modified and unmodified particles are stored at ambient temperature. Despite the
158 pH is not adjusted, the modified nanoparticles remain suspended in the mixture for 8 months.
159 As shown in Fig. 2(b), the modified Fe₃O₄ nanofluid is well dispersed in the vial, while
160 unmodified Fe₃O₄ nanofluid has precipitated down to the bottom of the vial. Fig. 2(a) presents
161 the TEM measurement of citric acid coated Fe₃O₄ nanoparticles.



162

163 **Fig. 1** (a) TEM measurement of bare Fe₃O₄ nanoparticles; (b) size distribution of bare Fe₃O₄
164 nanoparticles.

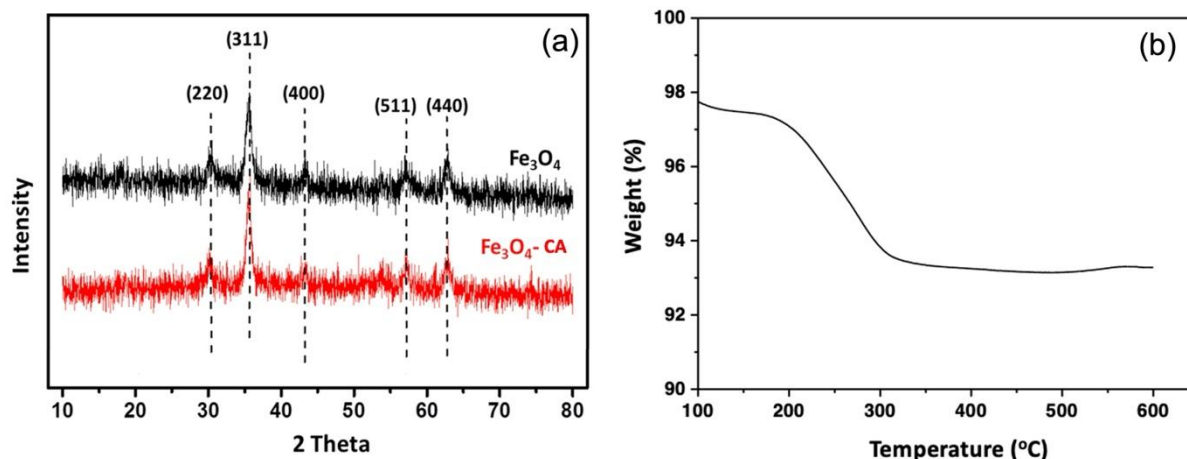
165



166

167 **Fig. 2** (a) TEM measurement of citric acid modified Fe_3O_4 nanofluid. (b) stability comparison
 168 between modified and unmodified water based nanofluids. (c) the schematic structure of the
 169 modified Fe_3O_4 nanoparticle.

170 There is no significant difference between modified and unmodified nanoparticles in shape
 171 and size. XRD pattern (Fig. 3(a)) presents the characteristic peaks of the cubic inverse spinel
 172 structure. The results show that there is no change in the crystal structure of Fe_3O_4
 173 nanoparticles, indicating that there are no detectable changes between modified and
 174 unmodified nanoparticles. TGA measurement suggests that the weight fraction of grafted
 175 citric acid is 4.2 % as shown in Fig. 3(b). The density of particles decreases to 4.36 g/cm^3 ,
 176 compared to that of unmodified particles, 4.51 g/cm^3 . It is known that the density of citric
 177 acid is 1.66 g/cm^3 . Thus, the volume fraction of citric acid modified is calculated to be 5.3%
 178 based on the densities of modified and unmodified particles and citric acid.

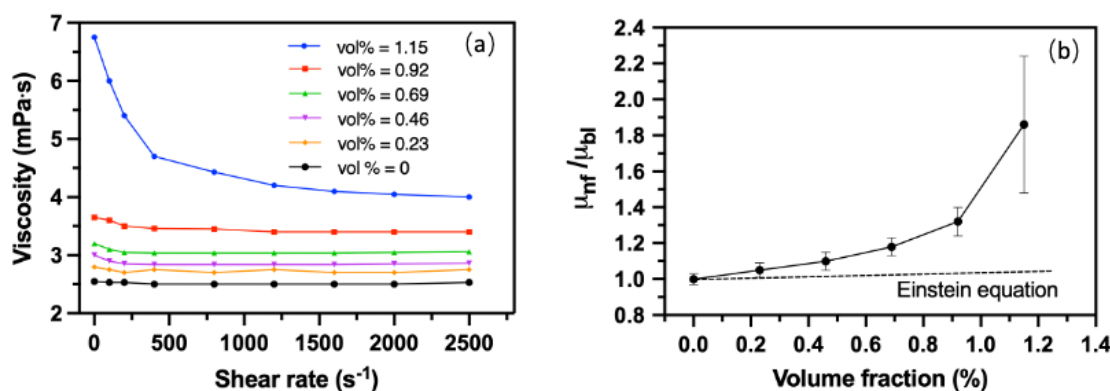


179
 180 **Fig. 3** (a) XRD characterisation of unmodified and modified Fe₃O₄ nanoparticles. (b) TGA
 181 characterisation of modified Fe₃O₄ nanoparticles.

182 **Viscosity of modified Fe₃O₄ nanofluid**

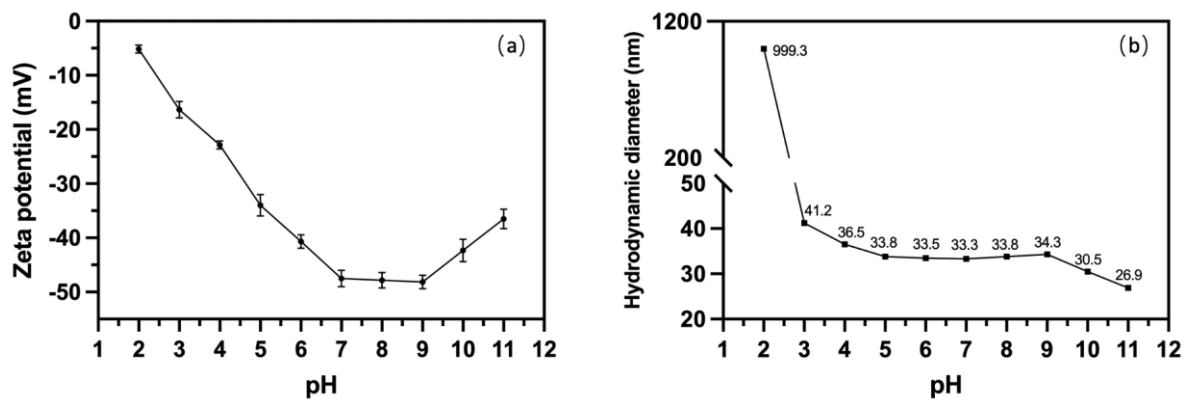
183 The viscosity of citric acid modified Fe₃O₄ nanofluid is investigated after nanoparticles are
 184 dispersed by ultrasonic treatment. The rheological behaviour is measured when the
 185 temperature is fixed at 30°C. Fig. 4(a) presents the effect of shear rate on the viscosity at
 186 different volume fractions. Except for the base liquid, all the nanofluids exhibit apparent shear
 187 thinning despite the particle volume fraction. For the volume fraction below 1%, the viscosity
 188 decreases by 4-6% as the shear rate reaches 2500 s⁻¹. The viscosity keeps decreasing with
 189 shear rate and a 40% decrease is found when the volume fraction exceeds 1%.

190 The pH value of Fe₃O₄ nanofluid is measured prior to rheological measurements and it keeps
 191 at 3-4 for all particle volume fractions. It is known that citric acid has three dissociation
 192 constants, which include pKa₁ = 3.13, pKa₂ = 4.76, and pKa₃ = 6.40, respectively. A pH of 3-4
 193 is supposed to hamper the dissociations of attached citric acid and hinders particle
 194 disaggregation as well. As shown in Fig. 4(b), the viscosity increases to 1.87 (± 20%) when the
 195 particle volume fraction reaches 1.15%, but experimental results show that the Einstein
 196 equation cannot predict the $\bar{\mu}$ of the prepared Fe₃O₄ nanofluid.



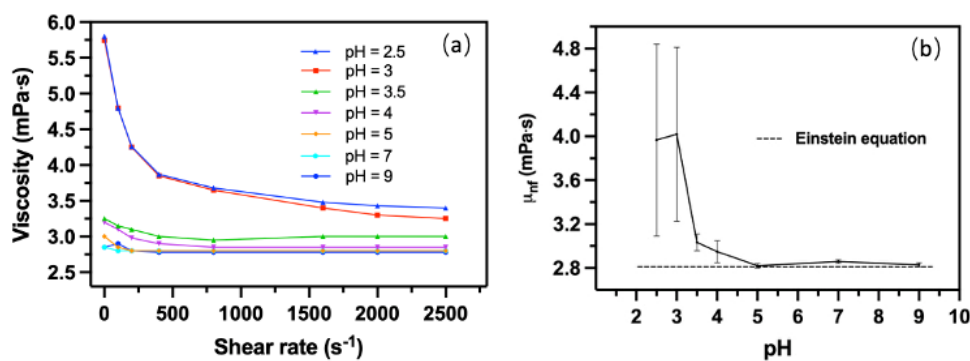
197
 198 **Fig. 4** (a) effect of the shear rate on citric acid modified Fe₃O₄ nanofluid at different particle
 199 volume fractions. (b) effect of volume fraction on the relative viscosity.

200 To investigate the disaggregation of modified Fe_3O_4 particles, DLS measurements are
 201 conducted at different pH values. Fig. 5 presents the zeta potential and hydrodynamic
 202 diameter of modified particles as a function of pH values. In Fig. 5(a), as the pH value increases
 203 to 7, zeta potential decreases quickly from -5.2 mV to -48.8 mV. When pH value comes to 7,
 204 8 and 9, zeta potential reaches the maximum range. At this range, particle disaggregation is
 205 promoted caused by the increase of the ionic strength of suspension due to the increase of
 206 Na^+ during the pH adjustment. When the pH value further increases to 11, although zeta
 207 potential comes to -36mV (Fig. 5(a)), the hydrodynamic diameter drops further to 26.9 nm
 208 (Fig. 5(b)). This phenomenon results from the increased ionic strength, which reduces the
 209 thickness of the electric double layer.



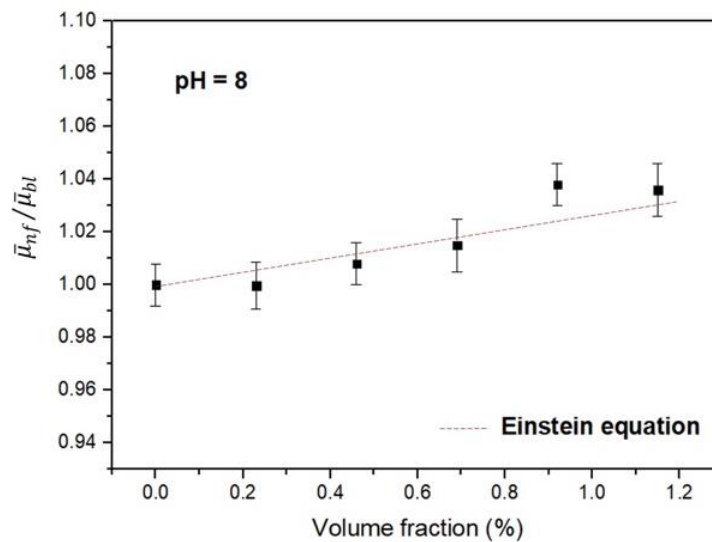
210
 211 **Fig. 5** (a) effect of pH on zeta-potential of modified Fe_3O_4 nanofluid. (b) effect of pH on DLS
 212 measurements of modified Fe_3O_4 nanofluid.

213 The viscosity of modified Fe_3O_4 nanofluids is also investigated at different pH values at 30°C .
 214 The particle volume fraction is fixed at 0.23%. As shown in Fig. 6(a), when pH value is at 5, 7
 215 and 9, the viscosity of modified Fe_3O_4 nanofluid does not change after the shear rate increase
 216 to 400 s^{-1} , nanofluid exhibits more like Newtonian fluid when the pH is raised up. Fig. 6(b)
 217 presents μ_{nf} as a function of the pH value. With the increase of pH, μ_{nf} decreases from 4.0
 218 ($\pm 22\%$) to 2.8 ($\pm 0.9\%$) mPa·s, which is consistent with the Einstein equation, and remains
 219 almost the same when pH is at 5, 7 and 9. Therefore, disaggregating nanoparticle is a feasible
 220 method to manipulate shear thinning and reduce the viscosity of the nanofluid.



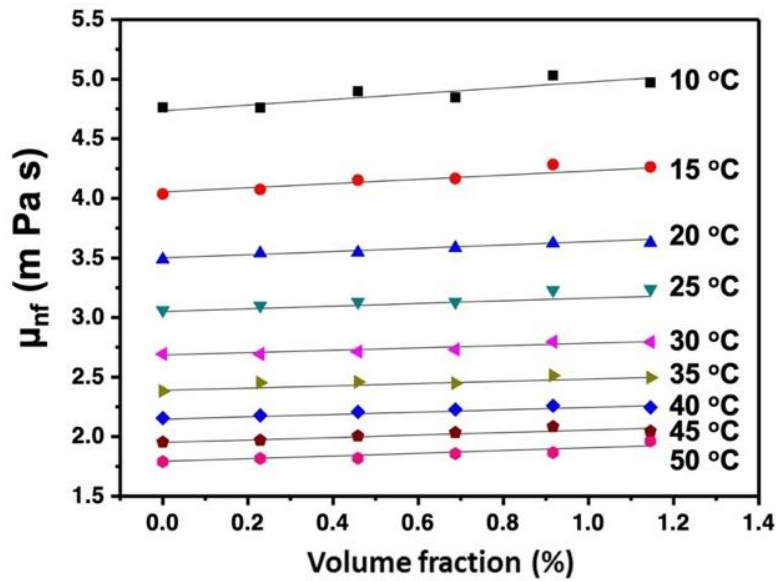
221
 222 **Fig. 6** (a) effect of shear rate on the viscosity of citric acid modified Fe_3O_4 nanofluids at
 223 different pH values. (b) effect of pH values on the viscosity of modified Fe_3O_4 nanofluid.

224 Furthermore, it is known that the pH value of a thermal working fluid needs to be carefully
 225 considered, this is because pH value has a direct impact on the corrosion of radiators and
 226 tubes. On one hand, an alkaline working fluid is more desired in engineering applications [25];
 227 on the other hand, according to the abovementioned experimental results, increased ionic
 228 strength caused by pH adjusting can reduce the surface potential of particles as shown in Fig.
 229 5(a). Consequently, a pH of 8 is selected for investigating the viscosity of modified Fe₃O₄
 230 nanofluid whose particles are highly dispersed. Fig. 7 presents the effect of relative viscosity
 231 on particle concentration at 30°C. The increment in the viscosity obeys the Einstein equation
 232 exactly with the maximum deviation of 1.6%. The amount of this increment is lower than
 233 reported results whose nanoparticles are disaggregated by only sonication [26].



234
 235 **Fig. 7** effect of particle volume fraction on the relative viscosity of modified Fe₃O₄ nanofluids
 236 at 30°C.

237 Moreover, at pH of 8, rheological measurements are also comprehensively carried out to
 238 investigate the relationship between experimental data of the viscosity of the modified Fe₃O₄
 239 nanofluid and the Einstein equation at different temperatures. Fig. 8 presents μ_{nf} as a
 240 function of volume fraction. The temperature of the measured sample ranges from 10 to 50 °C.
 241 As shown in Fig. 8, the solid line indicates the viscosity that is calculated by the Einstein
 242 equation. The experimental results show that data are in good agreement with the Einstein
 243 equation. The mean percentage difference is 1.3%. Therefore, when nanoparticles are highly
 244 disaggregated, the Einstein equation can accurately predict the viscosity of a Fe₃O₄ nanofluid.



245

246 **Fig. 8** viscosity of citric acid modified Fe_3O_4 nanofluid as a function of volume fraction at a
 247 fixed pH of 8 with the temperature from 10 to 50 °C. The solid line indicates the viscosity that
 248 is calculated by the Einstein equation.

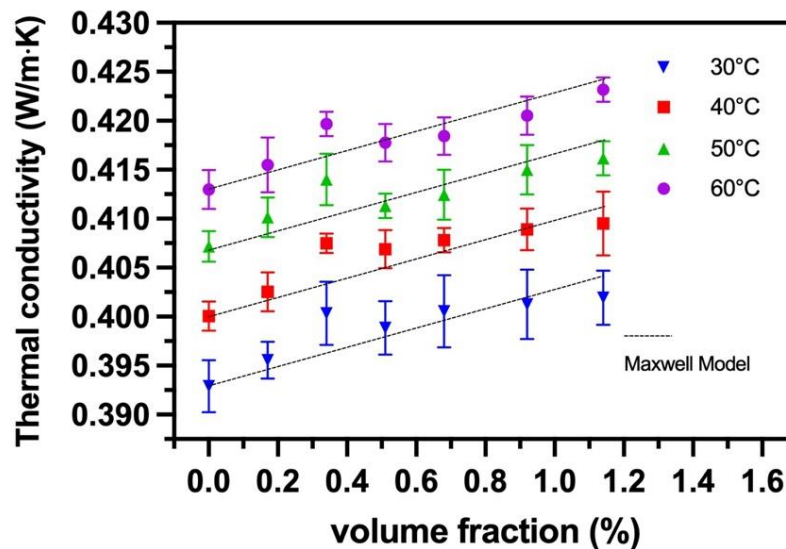
249 **Thermal conductivity of the modified Fe_3O_4 nanofluid**

250 The thermal conductivity of modified Fe_3O_4 nanofluid is also comprehensively investigated.
 251 The measured sample is required to preheat for 30 minutes for the thermal equilibrium. Fig.
 252 9 presents the effect of different temperatures and volume fractions on the thermal
 253 conductivity of modified Fe_3O_4 nanofluid. The pH value of modified Fe_3O_4 nanofluid all
 254 remains at 8. The volume fraction changes from 0 to 1.15%. The experimental results show
 255 that thermal conductivity increase with both temperature and volume fraction. When the
 256 volume fraction is at 1.15%, the enhancement of thermal conductivity increases by 2.2%, 2.3%,
 257 2.3% and 1.6%, when the temperature is at 30°C, 40°C, 50°C and 60°C, respectively. At present,
 258 there are several well recognised theories that can illustrate the enhancement mechanism of
 259 the thermal conductivity of nanofluid, which includes Brownian motion [27, 28], interfacial
 260 thermal resistance [29], the formation of solid-like 'nanolayer' on the nanoparticle surface
 261 [30-32] and thermal percolating paths due to nanoparticle aggregations [19, 20]. Bigdeli et al.
 262 et al [18] reported that there should be an optimum degree of aggregation for optimum
 263 thermal conduction of the nanofluid. Uncontrolled aggregations will result in the nanoparticle
 264 precipitation in solution, thus, thermal conduction only accounts for the base fluid. On the
 265 other hand, if nanoparticles are ideally disaggregated, there will be no thermal percolation
 266 paths formed to enhance the thermal conduction. Additionally, Prasher et al. [19] also
 267 supported that there should be an optimal nanoparticle aggregation range in order to obtain
 268 the optimal thermal conduction of nanofluid. They reported that the highly disaggregated
 269 nanofluid exhibited a thermal conductivity comparable to that predicted by the Maxwell
 270 model. Furthermore, the experimental results have proved that the thermal conductivity
 271 enhancement of the highly disaggregated nanoparticle suspension cannot be very significant
 272 [33]. Our experimental results, as shown in Fig. 9, are verified by the classic Maxwell model.

273 Thermal conduction of the modified nanofluid shows that there is no more different from a
 274 two-phase mixture when the prepared nanofluid exhibits a highly disaggregated condition.
 275 The measured thermal conductivity is consistent with the Maxwell model. The model can be
 276 described as follows,

$$277 \quad k_{nf} = k_{bl} \left[\frac{k_p + 2k_{bl} + 2\phi(k_p - k_{bl})}{k_p + 2k_{bl} - \phi(k_p - k_{bl})} \right]$$

278 The maximum deviation between the result calculated by the measured one and the Maxwell
 279 model is only 1.4%. Therefore, the Maxwell model can well predict the effective thermal
 280 conductivity of a two-phase mixture that consists of a continuous as well as discontinuous
 281 phase. Such a good match demonstrates that it is not necessary to consider the effects of the
 282 formation of solid-like “nanolayer”, interfacial thermal resistance and Brownian motion if the
 283 prepared nanofluid is kept in a highly disaggregated condition.



284
 285 **Fig. 9.** The effect of particle volume fraction and temperature on the thermal conductivity of
 286 modified Fe₃O₄ nanofluid at pH of 8. The dashed line represents the predicted value of the
 287 Maxwell model.

288 Conclusion

289 In this work, we study the effect of nanoparticle disaggregation on both viscosity and thermal
 290 conductivity of citric acid modified Fe₃O₄ nanofluid. Fe₃O₄ nanoparticles are coated with citric
 291 acid. By increasing the pH value of the nanoparticle suspension, the disaggregation of the
 292 nanoparticle is promoted because the surface potential becomes stronger due to the
 293 dissociation of the grafted carboxyl groups. The experimental results suggest that highly
 294 disaggregation is a feasible method for controlling the shear thinning and reducing the
 295 viscosity of Fe₃O₄ nanofluid. When Fe₃O₄ particles are highly dispersed, the viscosity of
 296 nanofluid does not change with the shear rate, and the viscosity is in good agreement with
 297 the Einstein equation. At temperatures ranging from 10 to 50°C, the average percentage
 298 difference between experimental data and the Einstein equation is only 1.3%. It is found that,

299 at the pH of 8, the thermal conductivity of highly dispersed nanofluid is consistent with the
300 classic Maxwell model, while the enhancement of the thermal conductivity of a highly
301 disaggregated nanofluid is relatively low. Small viscosity and better colloidal stability should
302 be competitive when nanofluid is considered for thermal engineering. Additionally, once
303 nanoparticles undergo uncontrolled aggregations, it could be difficult to predict the thermal
304 conductivity and viscosity at a specific temperature and particle concentration.

305

306 **Acknowledgement**

307 We would like to acknowledge the support of the RISE-ThermaSMART project, which has
308 received funding from the European Union's Horizon 2020 research and innovation program
309 under Marie Skłodowska-Curie Grant Agreement (No. 778104). The authors would also like
310 to acknowledge the support of China Scholarship Council (No. 201708060547).

311

312 **Reference**

- 313 1. Choi, S.U. and J.A. Eastman, *Enhancing thermal conductivity of fluids with*
314 *nanoparticles*. 1995, Argonne National Lab., IL (United States).
- 315 2. Philip, J., P. Shima, and B. Raj, *Enhancement of thermal conductivity in magnetite*
316 *based nanofluid due to chainlike structures*. *Applied physics letters*, 2007. **91**(20): p.
317 203108.
- 318 3. Farauo, J., J.S. Andreu, and J. Camacho, *Understanding diluted dispersions of*
319 *superparamagnetic particles under strong magnetic fields: a review of concepts,*
320 *theory and simulations*. *Soft Matter*, 2013. **9**(29): p. 6654-6664.
- 321 4. Chen, H., Y. Ding, and C. Tan, *Rheological behaviour of nanofluids*. *New journal of*
322 *physics*, 2007. **9**(10): p. 367.
- 323 5. Zhuang, J., et al., *Supercrystalline colloidal particles from artificial atoms*. *Journal of*
324 *the American Chemical Society*, 2007. **129**(46): p. 14166-14167.
- 325 6. Zhou, S.-Q., R. Ni, and D. Funfschilling, *Effects of shear rate and temperature on*
326 *viscosity of alumina polyalphaolefins nanofluids*. *Journal of Applied Physics*, 2010.
327 **107**(5): p. 054317.
- 328 7. Pastoriza-Gallego, M.J., et al., *Rheological non-Newtonian behaviour of ethylene*
329 *glycol-based Fe₂O₃ nanofluids*. *Nanoscale research letters*, 2011. **6**(1): p. 1-7.
- 330 8. Yu, W., et al., *Experimental investigation on thermal conductivity and viscosity of*
331 *aluminum nitride nanofluid*. *Particuology*, 2011. **9**(2): p. 187-191.
- 332 9. Pastoriza-Gallego, M.J., et al., *Rheological non-Newtonian behaviour of ethylene*
333 *glycol-based Fe₂O₃ nanofluids*. *Nanoscale research letters*, 2011. **6**(1): p. 560.
- 334 10. Prasher, R., et al., *Measurements of nanofluid viscosity and its implications for thermal*
335 *applications*. *Applied physics letters*, 2006. **89**(13): p. 133108.
- 336 11. Einstein, A., *Eine neue bestimmung der moleküldimensionen*. 1905, ETH Zurich.
- 337 12. Abareshi, M., et al., *Fabrication, characterization and measurement of thermal*
338 *conductivity of Fe₃O₄ nanofluids*. *Journal of Magnetism and Magnetic Materials*, 2010.
339 **322**(24): p. 3895-3901.

- 340 13. Sundar, L.S., M.K. Singh, and A.C. Sousa, *Thermal conductivity of ethylene glycol and*
341 *water mixture based Fe₃O₄ nanofluid*. International communications in heat and mass
342 transfer, 2013. **49**: p. 17-24.
- 343 14. Hamilton, R.L. and O. Crosser, *Thermal conductivity of heterogeneous two-component*
344 *systems*. Industrial & Engineering chemistry fundamentals, 1962. **1**(3): p. 187-191.
- 345 15. Azmi, W., et al., *The enhancement of effective thermal conductivity and effective*
346 *dynamic viscosity of nanofluids—a review*. Renewable and Sustainable Energy Reviews,
347 2016. **53**: p. 1046-1058.
- 348 16. Pang, C., et al., *Heat conduction mechanism in nanofluids*. Journal of Mechanical
349 Science and technology, 2014. **28**(7): p. 2925-2936.
- 350 17. Khanafer, K. and K. Vafai, *A critical synthesis of thermophysical characteristics of*
351 *nanofluids*. International Journal of Heat and Mass Transfer, 2011. **54**(19-20): p. 4410-
352 4428.
- 353 18. Bigdeli, M.B., et al., *A review on the heat and mass transfer phenomena in nanofluid*
354 *coolants with special focus on automotive applications*. Renewable and Sustainable
355 Energy Reviews, 2016. **60**: p. 1615-1633.
- 356 19. Prasher, R., P.E. Phelan, and P. Bhattacharya, *Effect of aggregation kinetics on the*
357 *thermal conductivity of nanoscale colloidal solutions (nanofluid)*. Nano letters, 2006.
358 **6**(7): p. 1529-1534.
- 359 20. Philip, J., P. Shima, and B. Raj, *Evidence for enhanced thermal conduction through*
360 *percolating structures in nanofluids*. Nanotechnology, 2008. **19**(30): p. 305706.
- 361 21. Shima, P., J. Philip, and B. Raj, *Role of microconvection induced by Brownian motion of*
362 *nanoparticles in the enhanced thermal conductivity of stable nanofluids*. Applied
363 Physics Letters, 2009. **94**(22): p. 223101.
- 364 22. Angayarkanni, S. and J. Philip, *Review on thermal properties of nanofluids: Recent*
365 *developments*. Advances in colloid and interface science, 2015. **225**: p. 146-176.
- 366 23. De Sousa, M.E., et al., *Stability and relaxation mechanisms of citric acid coated*
367 *magnetite nanoparticles for magnetic hyperthermia*. The Journal of Physical Chemistry
368 C, 2013. **117**(10): p. 5436-5445.
- 369 24. Liu, Z., et al., *Enhancement of solar energy collection with magnetic nanofluids*.
370 Thermal Science and Engineering Progress, 2018. **8**: p. 130-135.
- 371 25. Baboian, R. and G. Haynes, *Engine Coolant Testing: State of the Art*. ASTM
372 International, 1980.
- 373 26. Chiam, H., et al., *Thermal conductivity and viscosity of Al₂O₃ nanofluids for different*
374 *based ratio of water and ethylene glycol mixture*. Experimental Thermal and Fluid
375 Science, 2017. **81**: p. 420-429.
- 376 27. Jang, S.P. and S.U. Choi, *Role of Brownian motion in the enhanced thermal conductivity*
377 *of nanofluids*. Applied physics letters, 2004. **84**(21): p. 4316-4318.
- 378 28. Koo, J. and C. Kleinstreuer, *A new thermal conductivity model for nanofluids*. Journal
379 of Nanoparticle research, 2004. **6**(6): p. 577-588.
- 380 29. Nan, C.-W., et al., *Effective thermal conductivity of particulate composites with*
381 *interfacial thermal resistance*. Journal of Applied Physics, 1997. **81**(10): p. 6692-6699.
- 382 30. Jiang, H., et al., *Effective thermal conductivity of nanofluids Considering interfacial*
383 *nano-shells*. Materials Chemistry and Physics, 2014. **148**(1-2): p. 195-200.
- 384 31. Yu, W. and S. Choi, *The role of interfacial layers in the enhanced thermal conductivity*
385 *of nanofluids: a renovated Maxwell model*. Journal of nanoparticle research, 2003.
386 **5**(1): p. 167-171.

- 387 32. Yu, W. and S. Choi, *The role of interfacial layers in the enhanced thermal conductivity*
388 *of nanofluids: a renovated Hamilton–Crosser model*. Journal of Nanoparticle Research,
389 2004. **6**(4): p. 355-361.
- 390 33. Buongiorno, J., et al., *A benchmark study on the thermal conductivity of nanofluids*.
391 Journal of Applied Physics, 2009. **106**(9): p. 094312.
392